Decoupling chaotic amplification and nonlinear phase in high-energy thin-disk amplifiers for stable OPCPA pumping

Hanieh Fattahi,[1,2] Alexander Schwarz,[1,2] Xiao Tao Geng,[3,4] Sabine Keiber,[1,2] Dong Eon Kim[3,4], Ferenc Krausz[1,2], and Nicholas Karpowicz[1*]

[1]Max-Planck-Institut für Quantenoptik, Hans-Kopfermann-Straße 1, 85748 Garching, Germany
[2]Department of Physics, Ludwig-Maximilians-Universität München, Am Coulombwall 1, 85748 Garching, Germany
[3]Department of Physics, Center for Attosecond Science and Technology, Pohang University of Science and Technology, Pohang, 790-784, South Korea
[4]Max Planck Center for Attosecond Science, Pohang, 790-784, South Korea
[*]nicholas.karpowicz@mpq.mpg.de

Abstract: The dynamics of chirped pulse amplification in thin-disk regenerative amplifiers relevant to the pumping of optical parametric chirp pulse amplification systems are described. It is shown that the suitability for reproducible pumping of subsequent nonlinear processes requires a balance between the demands of avoiding chaotic pulse train dynamics and providing a reproducible spectral phase. We describe measures that may be taken to ensure that a laser system operates in the desired stable regime.

OCIS codes: (140.0140) Lasers and laser optics; (140.1540) Chaos; (140.3480) Lasers, diode-pumped; (140.3615) Lasers, ytterbium.

References and links

1. F. Krausz and M. I. Stockman, "Attosecond metrology: from electron capture to future signal processing," Nat. Photonics 8, 205–213 (2014).
2. H. Fattahi, H. G. Barros, M. Gorjan, T. Nubbemeyer, B. Alsaif, C. Y. Teisset, M. Schultze, S. Prinz, M. Haefner, M. Ueffing, A. Alismail, L. Vámos, A. Schwarz, O. Pronin, J. Brons, X. T. Geng, G. Arisholm, M. Ciappina, V. S. Yakovlev, D.-E. Kim, A. M. Azzeer, N. Karpowicz, D. Sutter, Z. Major, T. Metzger, and F. Krausz, "Third-generation femtosecond technology," Optica 1, 45 (2014).
3. A. Buck, M. Nicolai, K. Schmid, C. M. S. Sears, A. Sävert, J. M. Mikhailova, F. Krausz, M. C. Kaluza, and L. Veisz, "Real-time observation of laser-driven electron acceleration," Nat. Phys. 7, 543–548 (2011).
4. A. Dubietis, G. Jonušauskas, and A. Piskarskas, "Powerful femtosecond pulse generation by chirped and stretched pulse parametric amplification in BBO crystal," Opt. Commun. 88, 437–440 (1992).
5. H. Fattahi, C. Skrobol, M. Ueffing, Y. Deng, A. Schwarz, Y. Kida, V. Pervak, T. Metzger, Z. Major, and F. Krausz, "High efficiency, multi-mJ, sub 10 fs, optical parametric amplifier at 3 kHz," in Conference on Lasers and Electro-Optics 2012 (OSA, 2012), p. CTh1N.6.
6. T. Metzger, A. Schwarz, C. Y. Teisset, D. Sutter, A. Killi, R. Kienberger, and F. Krausz, "High-repetition-rate picosecond pump laser based on a Yb:YAG disk amplifier for optical parametric amplification," Opt. Lett. 34, 2123 (2009).
7. C. Teisset, M. Schultze, R. Bessing, M. Haefner, S. Prinz, D. Sutter, and T. Metzger, "300 W Picosecond Thin-Disk Regenerative Amplifier at 10 kHz Repetition Rate," in Advanced Solid-State Lasers Congress Postdeadline, G. and M. P. Huber, ed. (OSA, 2013), p. JTh5A.1.
8. M. Schulz, R. Riedel, A. Willner, T. Mans, C. Schnitzler, P. Russbueldt, J. Dolkemeyer, E. Seise, T. Gottschall, S. Hädrich, S. Duesterer, H. Schlarb, J. Feldhaus, J. Limpert, B. Faatz, A. Tünnermann, J. Rossbach, M. Drescher, and F. Tavella, "Yb:YAG Innoslab amplifier: efficient high repetition rate subpicosecond pumping system for optical parametric chirped pulse amplification.," Opt. Lett. 36, 2456–8 (2011).
9. C. Jauregui, J. Limpert, and A. Tünnermann, "High-power fibre lasers," Nat. Photonics 7, 861–867 (2013).
10. C. Hönninger, R. Paschotta, M. Graf, F. Morier-Genoud, G. Zhang, M. Moser, S. Biswal, J. Nees, A. Braun, G. A. Mourou, I. Johannsen, A. Giesen, W. Seeber, and U. Keller, "Ultrafast ytterbium-doped bulk lasers and laser amplifiers," Appl. Phys. B Lasers Opt. 69, 3–17 (1999).
11. J. Dörring, A. Killi, U. Morgner, A. Lang, M. Lederer, and D. Kopf, "Period doubling and deterministic chaos in continuously pumped regenerative amplifiers.," Opt. Express 12, 1759–68 (2004).

12. M. Grishin, V. Gulbinas, and A. Michailovas, "Bifurcation suppression for stability improvement in Nd:YVO4 regenerative amplifier.," Opt. Express 17, 15700–8 (2009).
13. M. Grishin, V. Gulbinas, and A. Michailovas, "Dynamics of high repetition rate regenerative," 15, 9434–9443 (2007).
14. M. D. Perry, T. Ditmire, and B. C. Stuart, "Self-phase modulation in chirped-pulse amplification," Opt. Lett. 19, 2149 (1994).
15. Y.-H. Chuang, L. Zheng, and D. D. Meyerhofer, "Propagation of light pulses in a chirped-pulse-amplification laser," IEEE J. Quantum Electron. 29, 270–280 (1993).
16. A. Antognini, K. Schuhmann, F. D. Amaro, F. Biraben, A. Dax, A. Giesen, T. Graf, T. W. Hänsch, P. Indelicato, L. Julien, C. Kao, P. E. Knowles, F. Kottmann, E. Le Bigot, Y. Liu, L. Ludhova, N. Moschüring, F. Mulhauser, T. Nebel, F. Nez, P. Rabinowitz, C. Schwob, D. Taqqu, and R. Pohl, "Thin-Disk Yb : YAG Oscillator-Amplifier Laser , ASE , and Effective Yb : YAG Lifetime," 45, 993–1005 (2009).
17. B. Chen, J. Dong, M. Patel, Y. Chen, A. Kar, and M. A. Bass, "Modeling of high-power solid-state slab lasers," in SPIE Proceeding, R. Scheps, ed. (2003), pp. 1–10.
18. U. Brauch, A. Giesen, M. Karszewski, C. Stewen, and A. Voss, "Multiwatt diode-pumped Yb:YAG thin disk laser continuously tunable between 1018 and 1053 nm," Opt. Lett. 20, 713 (1995).
19. M. Baumgartl, F. Jansen, F. Stutzki, C. Jauregui, B. Ortaç, J. Limpert, and A. Tünnermann, "High average and peak power femtosecond large-pitch photonic-crystal-fiber laser," Opt. Lett. 36, 244 (2011).
20. T. Eidam, J. Rothhardt, F. Stutzki, F. Jansen, S. Hädrich, H. Carstens, C. Jauregui, J. Limpert, and A. Tünnermann, "Fiber chirped-pulse amplification system emitting 3.8 GW peak power.," Opt. Express 19, 255–60 (2011).
21. A. Schwarz, M. Ueffing, Y. Deng, X. Gu, H. Fattahi, T. Metzger, M. Ossiander, F. Krausz, and R. Kienberger, "Active stabilization for optically synchronized optical parametric chirped pulse amplification," Opt. Express 20, 5557–5565 (2012).
22. J. Ratner, G. Steinmeyer, T. C. Wong, R. Bartels, and R. Trebino, "Coherent artifact in modern pulse measurements.," Opt. Lett. 37, 2874–6 (2012).
23. G. Arisholm, "General numerical methods for simulating second-order nonlinear interactions in birefringent media," J. Opt. Soc. Am. B 14, 2543 (1997).

1. Introduction

The generation of high energy, few-cycle laser pulses at a high repetition rate is of great interest, as progress in fields such as attosecond science [1,2] and high field physics [3] benefits directly from the availability of such sources. Optical parametric chirped pulse amplification (OPCPA) represents the most promising route to simultaneously achieving high pulse energies and large amplification bandwidths supporting intense, few-cycle pulses [4]. To push the frontiers of ultrafast pulse generation, pump lasers delivering sub-10 ps, high-energy pulses with near diffraction limited beam quality, ideally at repetition rates in the kHz to MHz range, are required [2,5].

Amplifiers based on Yb-doped gain media in disk [6,7], slab [8] or fiber [9] geometries are a most promising route as ytterbium has a broad absorption in a spectral region accessible by efficient laser diodes [6,10]. The long fluorescence lifetime of ytterbium makes it an ideal candidate for regenerative amplifiers as it supports substantial population inversion under continuous pumping. However, in continuously pumped regenerative amplifiers when the pulse repetition rate becomes comparable to the inverse of the gain relaxation time, bifurcation and chaotic pulse train dynamics can restrict the operating parameters of the laser system [11,12]. These instabilities can be suppressed by increasing the input seed energy to the regenerative amplifier [13], which may require additional stages of pre-amplification, or by increasing the pump intensity or number of passes of the pulse through the cavity, each of which may have negative consequences in terms of accumulation of nonlinear phase or intracavity power levels approaching the damage threshold of the optical elements. As a consequence, a regenerative amplifier may have excellent energy stability but exhibit variations in the temporal pulse shape that spoil the reproducibility of subsequent nonlinear processes [14,15]. It is therefore essential to both understand and manage these effects before a reliable OPCPA can be realized.

2. Theoretical description and experiment

In regenerative amplifiers operating at repetition rates close to the inverse of the inversion build-up time in the gain medium, the gain experienced by a pulse in the cavity is strongly coupled to the depletion caused by the previous pulse. This can result in nonlinear amplification dynamics, including both stable regimes such as period doubling (bifurcation) and chaotic regimes, where subsequent pulses exhibit extreme, seemingly random variations

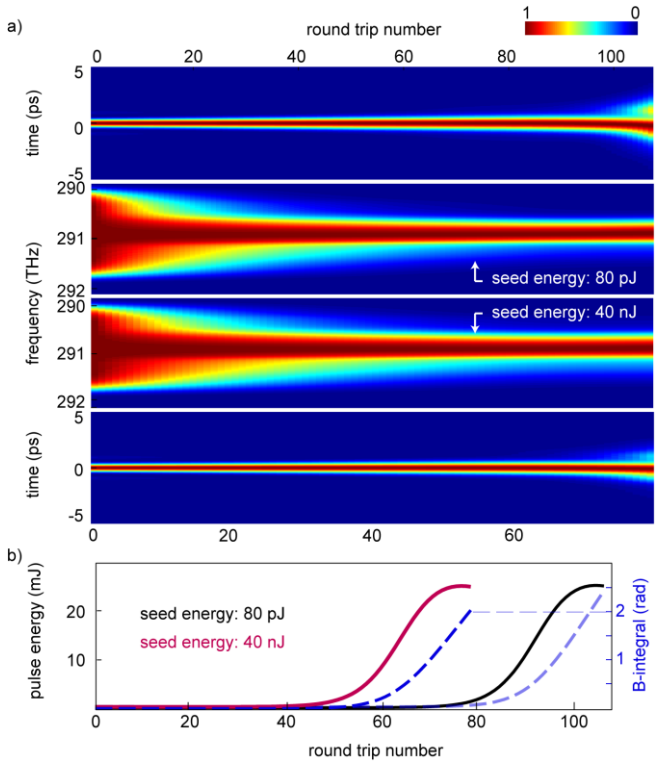

Fig. 1. (a) Simulated temporal and spectral profiles of the amplified pulses versus round trip number in a regenerative amplifier for two different input seed energy: 80 pJ and 40 nJ (amplitudes normalized). (b) Pulse build up in the regenerative amplifier for two different input seed energies, along with the build-up of B-integral in the cavity. The pulse distorts rapidly as the B-integral exceeds 2 for this output spectrum.

in energy. For example, consider the case of a pulse in a continuous-wave-pumped regenerative amplifier whose gain medium had been entirely depleted by the previous pulse. In the time between the exit of the previous pulse from the cavity and the entrance of the new pulse, the inversion in the medium was not sufficiently recovered to produce a high gain for the new pulse. As a result, its energy remains low for its time in the cavity, and it is unable to extract a significant amount of energy. By the time the next pulse comes, the inversion has recovered to a level where there is significant gain, the new pulse amplifies quickly and carries away a large amount of energy, leaving the medium depleted. This cycle then repeats, creating a stable energy bifurcation, with only every other pulse being amplified. If the inversion can recover to the same level between all pulses, the laser operates "normally", with each pulse entering the cavity exiting with the same energy. This can be ensured by increasing the number of round trips through the cavity, such that at a given seed and pump power level, each pulse will entirely deplete the medium.

In regenerative amplifiers with low input seed energy, a large number of round trips (passes through the gain medium) are required to reach energy saturation. This means a larger number of passes through the Pockels cell (PC) and air, increasing the accumulation of

nonlinear phase on the amplified pulses. This self-phase modulation (SPM) consequently influences the temporal and spectral shape of the pulse. In the SPM process the interference between the newly generated frequencies and the spectrum of the pulse causes a decrease or increase in the spectral bandwidth of the pulse. For heavily chirped pulses, however, SPM primarily influences the spectral phase of the pulse, leaving the shape of the spectrum unchanged. To study the effect of B-integral in low-energy-seeded regenerative amplifiers, a simple 1-D model propagating the gain medium inversion and wavelength-dependent pulse energy buildup for the full pulse train is developed, where the nonlinearity on the amplified pulse caused by the PC and air is calculated in each round trip. The populations in the ground and excited state manifolds are calculated based on the rate equations for continuously-pumped Yb:YAG [16] and the gain in each pass is obtained via the temperature-dependent emission cross-section according to [17].

The detailed simulation parameters are as follows: A seed pulse with 10 nm bandwidth is stretched using 1.19×10^{8} fs^{2} dispersion, to approximately 2 ns. After entering the cavity, the pulse travels 40 ns in each round trip, with a beam waist of 3.4 mm ($1/e^{2}$) on the 20-mm-long PC (twice per round trip), similar to [6] and with an assumed nonlinear refractive index of 2.99×10^{-20} cm^{2}/W. The nonlinearity of the gain medium is neglected as it is small compared to that of the PC. 225 W of pump power with a 2.8 mm beam waist is used to pump the 100-µm-thick gain medium with 12.5% doping and 1.2 ms upper state lifetime, with the assumption of 90% absorption of the incident pump light and 95.5% overlap of the pumped energy with the cavity mode. The Yb:YAG temperature is 300 K, and the emission spectrum as determined by [18] is used to determine the spectral profile of the gain. The mode of the seed is assumed match that of the cavity. The cavity round trip transmission efficiency is 98% and each trip takes 40 ns. The repetition rate is set to 3 kHz, such that the inversion rebuilds under constant pumping conditions for 333 µs between pulses. The pulse passes twice through the disk during each round trip. The SPM is calculated in each round trip so that SPM-induced spectral changes will influence the gain and efficiency of the amplifier. The simulation is run over 120 pulses in the pulse train to reach a steady state. The same parameters are used in all calculations.

The calculation is shown in Figure 1 for two input seed energies, 80 pJ and 40 nJ. Fig. 1 compares the pulse build up and spectral and temporal behavior of the amplified pulses for these two cases. For 80 pJ seed energy, 107 round trips are required to reach saturation. At this number of the round trips, the accumulated B-integral causes undesired higher-order nonlinear phase on the amplified pulses, which makes the compression of the pulse to its Fourier transform limit challenging. The spectral narrowing versus the round trip number visible in Fig. 1 is caused by the limited gain bandwidth of the medium. Increasing the input seed energy to 40 nJ will reduce the required number of round trips to reach saturation to 90. In this case the introduced nonlinear phase on the pulse is negligible and leaves the temporal phase of the pulse well-behaved. The difference is due to two factors: the reduced nonlinear path through the regenerative amplifier, and more significantly, the reduction of gain narrowing, which results in a longer pulse inside of the cavity after amplification to high energy, and a correspondingly lower intensity. When the B-integral exceeds approximately 2, the pulse rapidly distorts. This, combined with the fact that the rate of increase of the nonlinear phase is maximized when the amplifier reaches energy saturation, has the end result that there is a sharp threshold where nonlinear phase fluctuations may easily exceed energy fluctuations as a source of changes in the peak power of the laser output. The exact pulse deformation depends on the spectral profile of the amplified light – with linear chirping, the profile of the spectral intensity is imprinted onto the spectral phase.

A Yb:YAG thin-disk regenerative amplifier as described in [6], is used for experimental verification of these effects in this study. In this system, the 1 pJ pulses centered at 1030 nm, driven from a Ti:sapphire oscillator were amplified to 80 pJ exploiting a diode-pumped, fiber

pre-amplifier [9,17,18]. A second fiber pre-amplifier was placed after the pulse picker for further amplification of seed pulses up to 40 nJ. At the seed energy level of 80 pJ and 107 cavity round trips, after intermediate chaos period doubling and stable regime of operation was achieved resulting in 20 mJ pulse energy at 3 kHz repetition rate after passing through a grating pair for temporal compression. The SHG-FROG measurement indicates that the accumulated nonlinear phase, due to the large number of round trips, distorted the temporal phase of the amplified pulse, without affecting the spectrum.

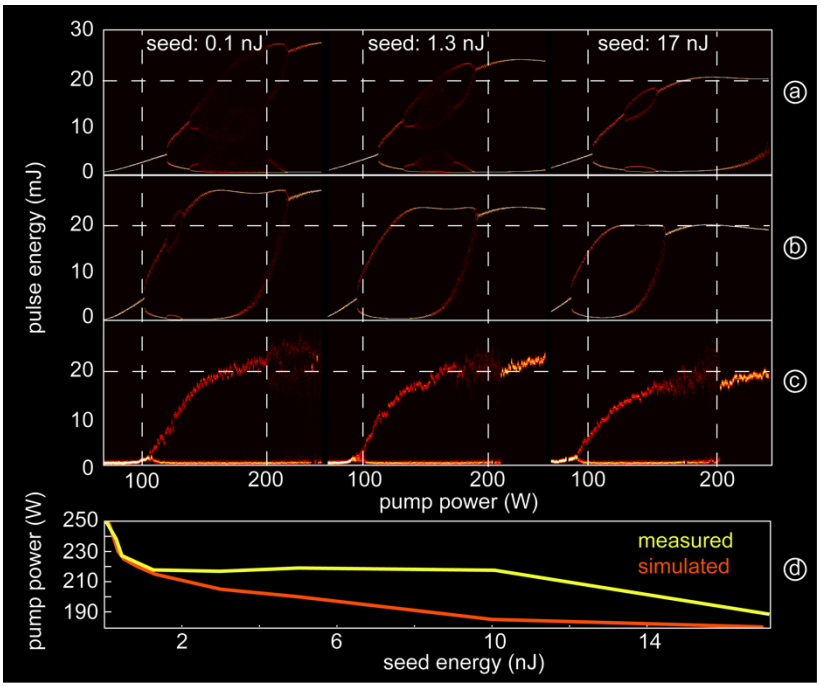

Fig. 2. Simulated and measured pulse train dynamics for CW-pump Yb:YAG thin-disk amplifiers for varying seed levels and repetition rates. (a) Simulated pulse train dynamics at 6 kHz Pockels cell rate, exhibiting chaotic behavior at low seed energies and stable bifurcation at higher pump powers. (b) The same system simulated at 3 kHz, showing the elimination of chaos at all powers and the removal of bifurcation at higher pump powers. (c) Measured dynamics at 3 kHz. (d) Required pump power for stable operation as a function of pulse energy at 3 kHz.

By increasing the input seed energy, a stable regime of operation with no chaotic behavior and no period doubling was observed. Figure 2 shows the energy distribution in a bifurcation diagram acquired by incrementing the pump power over the range of 50–250 W with the number of round trips in the amplifier being kept constant at 100. For a cavity seeded with 0.1 nJ of energy, at 100 W of pump power, bifurcation occurred while the PC was driven at 3 kHz repetition rate. Increasing the pump power to 250 W lead to repetition rate preserving amplification. Increasing the input seed energy shifted both the bifurcated and normal amplification points to lower pump powers. The measured data are consistent with the simulation, indicating no chaotic behavior for the case of high energy seeding. In the case of 6 kHz operation, chaotic behavior appears, as measured in [6], resulting from the stronger pulse-to-pulse coupling. Period doubling persists to higher pump powers, and reaches a stable doubling regime, whose location and separation from chaotic zones is determined by the seed energy. Under the same conditions, when the PC is operated at 6 kHz in period doubling, normal operation may be obtained with the PC run at 3 kHz, reducing the thermal load on the PC crystal and simplifying synchronization with OPCPA seed sources [21]. It is noteworthy that the severity of the nonlinear cavity dynamics decreases as the seed level increases; this is

due to the reduced sensitivity of the amplification to the process to the degree of inversion of the medium with decreased gain. This has the end result that wider range of stable operating points is available with higher seed levels, making it more likely that a mode with low B-integral and the desired repetition rate can be found.

The primary difference between the simulation and the experiment is in the tendency of the laser to emerge from bifurcation and stay in the normal operation regime even if the pump power is slightly reduced (hysteresis), due to the fact that the cavity is optimized for high-power operation, including thermal effects not present in the simulation: the cavity efficiency increases slightly as the system enters the normal amplification mode and the output power doubles.

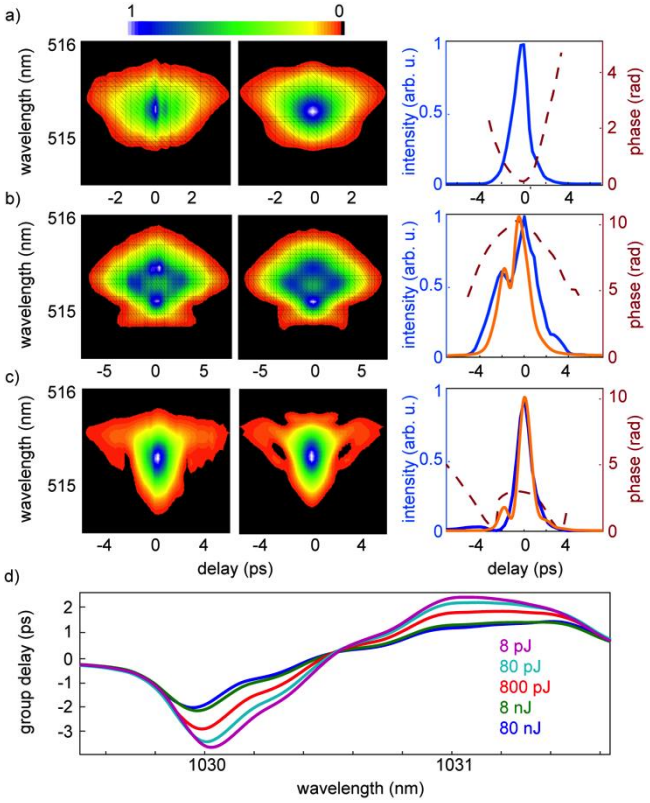

Fig. 3. Pulse dynamics in regenerative amplifier exhibiting SPM and its removal. (a) unsaturated SHG-FROG trace using 80 pJ seed amplified to 14 W (unstable laser output in the unsaturated regime). (b) 80 pJ seed amplified to 58W, exhibiting strong SPM. (c) 300 pJ seed amplified to 61 W with increased pump power and reduced round trips, exhibiting minimal SPM. (d) Additional group delay resulting from nonlinear phase as calculated for varying seed levels, with sufficient number of round trips to reach saturation.

Fig. 3 shows how the cavity dynamics affect the temporal profile of the compressed pulse. In Fig. 3(a) the unsaturated output of a laser system seeded with 80 pJ, amplified to 14 W shows a nearly transform-limited profile, but after increasing the energy to 58 W in Fig. 3(b), the pulse is obviously distorted by SPM. After increasing the seed energy to just 300 pJ and reducing the round trip number by 10 (combined with additional pump power) the compressed pulse characterized with a SHG-FROG indicates a good temporal profile for the pulse (i.e. SPM effects are negligible), at an average power of 61 W (Fig. 3(c)). A sufficient amount of pre-amplification of pJ-level seed pulses is therefore essential for the reproducibility of the peak power produced by the amplifier. In Fig. 3(d), the numerical results showing the effect of seed energy on the nonlinear group delay distortion of the output pulses are shown, explaining the difference in the three FROG traces. Additionally, the trace

in Fig. 3(b) reconstructs with significantly more G-error than the corrected trace in Fig. 3(c), 0.022 compared to 0.0087, respectively. This may indicate pulse-to-pulse variations in shape [22].

The elimination of SPM effects can be attempted via several approaches, some entailing compromises in other areas of laser performance or system complexity. A number of possible approaches, along with their mechanisms and drawbacks are shown in Table 1, in order of approximate overall difficulty. As opposed to lasers exhibiting no chaotic behavior, the simple solution of reducing the pump intensity does not work for these systems: the laser must operate with both a stable pulse train (at the correct repetition rate) and have a clean spectral phase. This can only be accomplished by decoupling the pulse distortion of the pulse from the nonlinear pulse train dynamics by the use of methods that do not affect both characteristics to the same degree.

Table 1. Possible approaches to the reduction of SPM in a thin disk regenerative amplifier

Approach	Mechanisms	Negative consequences
Reduce round trips with higher pump power	- Reduced nonlinear path length - Reduced cavity losses leading to less gain narrowing at same energy	- Increased thermal load - Smaller range of stable operating power
Increase seed level via further broadband pre-amplification	- Reduced gain narrowing - Reduced nonlinear propagation distance via reduced round trip number	- Increased system complexity/cost - Longer seed beam path
Decrease pump spot size	- Faster inversion buildup for given pump power, allowing stable operation at lower power	- Increased thermal gradient in gain medium - Reduced saturation energy
Increase stretcher and compressor dispersion	- Reduced intensity at given pulse energy	- Increased cost and alignment sensitivity of compressor and stretcher - Additional timing jitter when synchronized with external seed
Increased beam size in nonlinear cavity elements via reflective telescope	- If a single element (i.e. Pockels cell) is responsible, reduced intensity	- Increased complexity of the laser cavity - Requires larger cavity optics
Operation in vacuum	- Reduced nonlinearity of free beam path	- Cost and complexity - More difficult thermal management

3. Effect of suboptimal amplifier design on OPCPA

In the event that significant SPM can be observed in the pulse emitted from such an amplifier, it is likely that it cannot be used reproducibly until it is eliminated, e.g. by the design changes listed above. In the case of significant SPM, small changes in the seed and cavity alignment result in large variations of the output of an OPCPA pumped by such a pulse. These effects are shown in Fig. 4, where pulses with the same energy and spectrum, but with varying levels of SPM result in significant variations in the efficiency and spectrum of the pulses amplified in a broadband OPCPA. As a result, even in the total absence of energy fluctuations in the output of a saturated amplifier, variations of the spectral phase induced by the sensitivity of the SPM process to the evolution of the pulse inside of the cavity can nevertheless result in large fluctuations in the OPCPA.

This is shown in the simulations presented in Fig. 4, calculated using the SISYFOS 3D code [23]. In the simulation, 20-mJ, 1030-nm pump pulses with the beam diameter of 3.3 mm at full width half maximum are used to amplify a broad spectral range in a single OPCPA stage. The OPCPA consists of a 2.7 mm-thick $LiNbO_3$ crystal with d_{eff} value of 3.3 pm/V, and a phasematching angle of 45.25º. Here the broadband phasematching is fulfilled as the OPA works in degeneracy. Seed pulses with the energy of 3 μJ and the beam diameter of 3.3 mm

are considered. The pulses from Fig. 3 (b)-3 (c) are used as the temporal profile of pump pulses in the simulation whereas a super-Gaussian of the order of four is assumed for the seed in the time domain. The 1.6-ps seed pulses are linearly chirped in both cases. The thickness of the $LiNbO_3$ crystal is optimized to reach gain saturation in the OPCPA when the temporal profile of pump is taken from the measurement shown in Fig. 3 (c). Using identical parameters for OPCPA and pump pulses with accumulated nonlinear phase (Fig. 3 (b)), results in a factor of 3.5 difference in amplified energy and decreases the conversion efficiency from 12% to 2.2%. Here the OPA does not reach gain saturation anymore and the amplified spectrum becomes modulated in consistent with the temporal shape of the pump pulses.

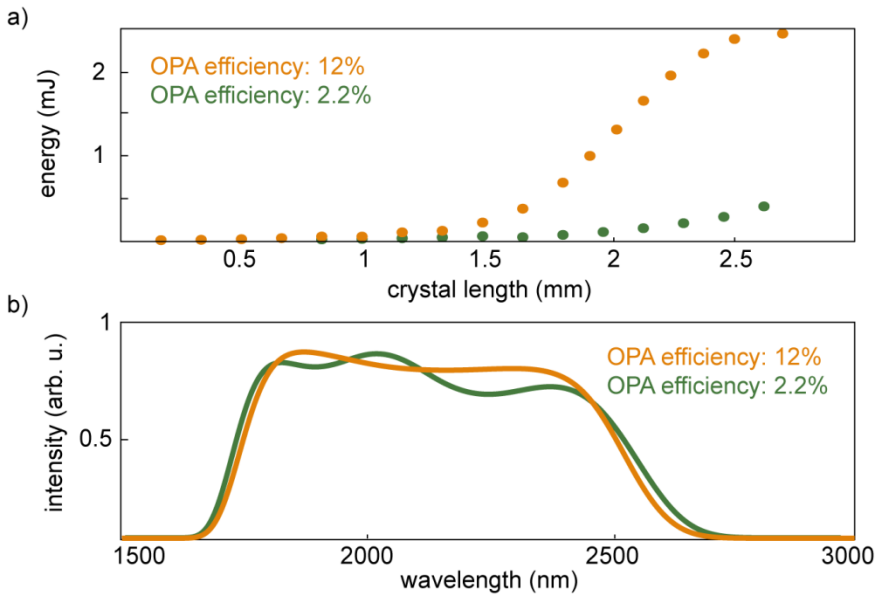

Fig. 4. Simulation of the effects of amplifier SPM on the output of a broadband OPCPA. Orange curves are simulated with the pulse measured in Fig. 3 (c) and green curves with the pulse in Fig. 3 (b), all other parameters are the same: pump energy 20 mJ, seed energy 3 µJ amplified in 2.7 mm $LiNbO_3$ with the phasematching angle 45.25°. (a) Gain vs. crystal length in the OPCPA, showing saturation with the SPM-free pulse, and a factor of 3.5 reduction in pulse energy with the distorted pump pulse. (b) Modification of the spectrum resulting from the pump temporal profile (normalized).

4. Conclusion

Stable OPCPA demands not only excellent pump energy stability, but also a high degree of reproducibility of the temporal shape of the pump pulses, which can only be ensured by careful matching of the amplifier design to the seed specifications. The relevant effects can be modeled and understood using a simple numerical approach, which when combined with an awareness of the various trade-offs involved, allows an optimal design for a given set of inputs and target parameters. By ensuring that these effects are well controlled, thin-disk regenerative amplifiers are an ideal route to stable and efficient pumping of high-power, high-energy broadband OPCPAs, enabling the exploration of new frontiers in ultrafast science.

Acknowledgments

We gratefully acknowledge helpful discussions with Gunnar Arisholm and valuable technical support from the group of Jens Limpert and also support from LASERLAB-EUROPE (grant agreement no. 284464, EC's Seventh Framework Programme), the Munich-Centre for

Advanced Photonics, and the German Federal Ministry of Education and Science (BMBP) via the NEXUS project. Dong Eon Kim and Xiao Tao Geng thank the support from Global Research Laboratory Program [Grant No 2009-00439] and Max Planck POSTECH/KOREA Research Initiative Program [Grant No 2011-0031558] through the National Research Foundation of Korea (NRF) funded by Ministry of Science, ICT & Future Planning.